Environmental Science Nano

House Dust Mite Extract Forms a Der p 2 Corona on Multi-Walled Carbon Nanotubes: Implications for Allergic Airway Disease

Journal:	*Environmental Science: Nano*
Manuscript ID	EN-ART-09-2023-000666.R1
Article Type:	Paper

Environmental Significance

Multi-walled carbon nanotubes (MWCNTs) are used in materials essential for the construction, automotive, and aerospace industries. Workers are exposed to these engineered nanomaterials during manufacturing. Consumers are exposed following environmental release of the materials. Inhalation is of specific concern as the major route of exposure in both the occupational and environmental setting. In 2013, the National Institute for Occupational Safety and Health (NIOSH) provided an overview of the occupational hazards associated with these materials and recommended exposure limits. Real-world human exposure will likely not be limited to pristine MWCNTs. A variety of organic and inorganic substances can adsorb on MWCNTs. For example, various types of air pollution and allergens will also be inhaled with the MWCNTs. Our research examined the complex interaction of MWCNTs, house dust mite allergens, and lung fluid proteins. By providing a detailed molecular characterization of this interaction, we hope to better understand observed increases in allergic airway disease caused by co-exposures to nanomaterials and allergens.

House Dust Mite Extract Forms a Der p 2 Corona on Multi-Walled Carbon Nanotubes: Implications for Allergic Airway Disease

Judith Dominguez,[a] Samantha K. Holmes,[a] Ryan D. Bartone, [b] Logan J. Tisch,[b] Robert M. Tighe,[c] James C. Bonner,[b] Christine K. Payne[a,*]

*christine.payne@duke.edu

a. Thomas Lord Department of Mechanical Engineering and Materials Science, Duke University, Durham, North Carolina, USA 27708
b. Toxicology Program, Department of Biological Sciences, North Carolina State University, Raleigh, North Carolina, USA 27695
c. Department of Medicine, Duke University School of Medicine, Durham, North Carolina, USA 27710

Abstract

Multi-walled carbons nanotubes (MWCNTs) are used in materials for the construction, automotive, and aerospace industries. Workers and consumers are exposed to these materials via inhalation. Existing recommended exposure limits are based on MWCNT exposures that do not take into account more realistic co-exposures. Our goal was to understand how a common allergen, house dust mites, interacts with pristine MWCNTs and lung fluid proteins. We used gel electrophoresis, western blotting, and proteomics to characterize the composition of the allergen corona formed from house dust mite extract on the surface of MWCNTs. We found that the corona is dominated by der p 2, a protein associated with human allergic responses to house dust mites. Der p 2 remains adsorbed on the surface of the MWCNTs following subsequent exposures to lung fluid proteins. The high concentration of der p 2, localized on surface of MWCNTs, has important implications for house dust mite-induced allergies and asthma. This research provides a detailed characterization of the complex house dust mite-lung fluid protein coronas for future cellular and *in vivo* studies. These studies will help to address the molecular and biochemical mechanisms underlying the exacerbation of allergic lung disease by nanomaterials.

Introduction

Multi-walled carbons nanotubes (MWCNTs) are essential components of electronics, plastics, sensors, and coatings with applications in the construction, automotive, and aerospace industries.[1, 2] Given this wide range of applications, it is important to understand the effects that MWCNTs may have on both workers in the manufacturing setting and consumers who are exposed to these materials following environmental release. Inhalation is of specific concern as this is the primary route of exposure.[3-6] The pulmonary toxicity of MWCNTs in rodents is well-demonstrated and known to be dependent on the physicochemical characteristics of the MWCNTs.[7-14] For example, rigid, rod-like MWCNTs are more toxic than flexible, tangled, MWCNTs.[15] The National Institute for Occupational Safety and Health (NIOSH) provides an overview of the occupational hazards associated with these materials and recommended exposure limits.[16] These recommended exposure limits are based solely on MWCNT exposure that do not take into account more realistic co-exposures. For example, allergic lung disease induced by common allergens, such as those from house dust mites (HDM; *Dermatophagoides pteronyssinus*), is exacerbated by MWCNT inhalation exposure in mice.[17] These findings suggest that the current exposure limits to MWCNTs should take into account co-exposures. In addition, the mechanistic details underlying the observed toxicity of these nanomaterial-allergen co-exposures are lacking, especially regarding the initial steps of inhalation and the relationship of material properties to physiological and pathological outcomes.[18, 19]

Previous work has shown that blood serum proteins and cell lysates adsorb on the surface of MWCNTs forming a protein corona.[20-23] The protein corona, rather than the bare nanomaterial, determines the subsequent biological events including cellular internalization and immune response.[24-30] Our research focuses on the formation of an allergen corona as MWCNTs interact with allergens in the environment, followed by the interaction of these allergen-MWCNTs with lung fluid obtained from mice. The interaction of titanium dioxide and polystyrene nanoparticles with bronchoalveolar lavage fluid (BALF) has been characterized previously.[31, 32] For the titanium dioxide nanoparticles, a BALF corona led to increased expression of pro-inflammatory cytokines in macrophages.[32] To the best of our knowledge, our work described below is the first to address a combined allergen and lung fluid corona.

We examine one common allergen, HDM extract. Allergies to HDM are estimated to affect 1-2% of the global population.[33-35] Eighty-five percent of asthmatics are allergic to HDM.[36] HDM extract is a multi-component allergen consisting of a mixture of proteins from mites, nymphs, fecal matter, and eggs.[37-40] Of specific interest are two proteins, der p 1 and der p 2.[38] The majority (~80%) of people with HDM allergies are sensitive to der p 1 and der p 2.[41] Sera samples from allergic subjects showed that 50% of IgE binding was directed at these two proteins.[42] Der p 1 is a cysteine protease.[43-46] Der p 2 is a myeloid differentiation factor-2-related lipid recognition domain lipid-binding family protein,[47] which is found in the digestive track and feces of HDM.[48] Previous work has suggested that a HDM corona on MWCNTs could be a factor in the exacerbated allergic airway disease observed in mice.[49] Proteolytic assays showed that the der p 1-gold nanoparticle

conjugates had increased proteolytic activity compared to der p 1,[50] suggesting that allergen coronas may amplify allergic responses. This is supported by *in vivo* experiments showing that mice co-exposed to MWCNTs and HDM displayed increased allergic lung inflammation that was not observed with MWCNTs or low doses of HDM alone.[17]

In terms of human exposures, MWCNTs could encounter HDM in both manufacturing and consumer settings. HDM are ubiquitous in the indoor environment: They thrive in upholstered furniture, carpets, bedding, and dust. Previous work has found that MWCNTs were present in the office areas adjacent to production facilities.[51] In these office areas, MWCNTs would certainly come into contact with HDM. This study did not measure HDM in the MWCNT production facility, but it is likely that such facilities also contain some HDM, especially in production areas that may contain dust. It is also possible that MWCNTs and HDM will come into contact during the life cycle of the nanomaterial, where there is release of MWCNTs from a matrix or during recycling.[52] For example, the future use of MWCNTs in textiles would result in consumer exposure within homes that contain HDM. *In vitro* experiments examined gold nanoparticles (50 nm) conjugated to der p 1.[50]

Our approach, described below, was to characterize the protein corona formed on MWCNTs incubated with HDM extract, both alone and in combination with BALF. We focus on a single type of MWCNT (NC7000), which is the parent nanomaterial that can be further chemically or thermally purified and functionalized.[14] We use gel electrophoresis, western blotting, and proteomics to characterize the composition of the protein corona. We found that HDM extract forms a corona on the surface of MWCNTs and that this corona is dominated by der p 2. Der p 2 remains adsorbed on the MWCNTs following subsequent exposures to BALF or albumin, the main protein present in BALF. The high concentration of der p 2, localized on surface of MWCNTs, has important implications for HDM-induced allergies and asthma. This research will help to address the molecular and biochemical mechanisms underlying the exacerbation of allergic lung disease by nanomaterials and provides a detailed characterization of these complex protein coronas for future cellular and *in vivo* studies.

Materials and Methods

MWCNT characterization

MWCNTs (NC7000, Nanocyl, Sambreville, Belgium) were used for all experiments. Stock solutions of MWCNTs were prepared by suspending dry MWCNTs (10 mg/mL) in 1X phosphate buffered saline (PBS; 21300025, Thermo Fisher, Waltham, MA). Solutions were sonicated for five minutes with a cup horn sonicator (40% amplitude; Q500 Sonicator, Q Sonica, Newtown, CT) to help suspend the MWCNTs.

Transmission electron microscopy (TEM; Talos F200X, Thermo Fisher) was used to quantify the diameter of the MWCNTs. A MWCNT solution (100 µg/mL in PBS) was drop-cast onto carbon coated copper grids (FCF200-Cu, Electron Microscopy Sciences, Hatfield, PA). Images were collected with 50 kX magnification at 200kV. ImageJ was used for image analysis.[53] X-ray photoelectron spectroscopy (XPS; Kratos Analytical Axis Ultra, Shimadzu Corporation, Kyoto, Japan) at the Shared Materials Instrumentation

Facility at Duke University was used to measure the elemental composition of the MWCNTs.

Rodent bronchoalveolar lavage fluid (BALF)

Our procedure for obtaining BALF has been described previously.[32] All procedures were approved by the Duke University Institutional Animal Care and Use Committee (IACUC) and were performed under an IACUC approved animal protocol (A053-21-03). All animal experiments were conducted in accordance with the American Association for the Accreditation of Laboratory Animal Care guidelines. In brief, C57BL/6 male mice (8-10 weeks) were purchased from Jackson Laboratories (Bar Harbor, ME). Bronchoalveolar lavages were performed following a published protocol.[45] Prior to lavage, mice were deeply anesthetized with an intraperitoneal injection of ketamine (100 mg/kg), xylazine (100 mg/kg), and saline (0.9%), dosed by weight (350-500 µL). The chest and trachea were dissected to expose the lungs and trachea. Tubing (PE-60, #9565S30, Thomas Scientific, Swedesboro, NJ) was inserted into the trachea and attached to a 12-inch infusion set (#SV-25BLK, Terumo, Tokyo, Japan) connected to a 10 mL syringe held on a ring stand. Lungs were passively filled to 20 cm H_2O with PBS to reach total lung capacity. The BALF was then passively drained and placed on ice for further processing. BALF used for protein corona formation was pooled from 10-20 mice to reduce mouse-to-mouse variation.

Protein corona formation and concentration

Protein coronas were formed by incubating MWCNTs with proteins for 30 minutes at room temperature (RT) on an orbital shaker (700 rpm, 88882006, Digital Microplate Shaker, Thermo Fisher). Proteins used included HDM (*Dermatophagoides pteronyssinus*, XPB91D3A2.5, Lot 414145, Stallergenes Greer, Lenoir, NC), bovine serum albumin (BSA; A2153-50G, Sigma-Aldrich, St. Louis, MO), and BALF. To remove unbound protein, samples were washed three times by centrifugation (15-30 minutes, 4 °C, 14,000 rpm) and resuspension in PBS. Removal of unbound and weakly proteins results in a "hard" corona. To create sequential coronas, the corona formation procedure was repeated using a second protein. Protein concentrations were measured with a colorimetric assay (Pierce 660 nm Protein Assay, referred to as a 660 nm assay, 2260, Thermo Fisher Scientific) and quantified with a plate reader (SpectraMax iD3, Molecular Devices, San Jose, CA).

Gel electrophoresis

The compositions of the protein coronas were visualized using gel electrophoresis. Protein-MWCNT complexes were resuspended in Laemmli SDS-Sample Buffer (4X, Reducing, BP-110R, Boston BioProducts, Milford, MA). Proteins were denatured by boiling samples at 95°C for 5 minutes before loading into a tris-glycine sodium dodecyl sulfate (SDS) precast polyacrylamide gel (4561096, Bio-Rad Laboratories, Hercules, California). A 10-250 kDa molecular weight marker (Precision Plus Protein Dual Color Standards, 1610374, Bio-Rad) was included in the gel. A voltage of 230 V was applied for 30 minutes. The gel was rinsed by microwaving in deionized water three times (1 minute heat, 1 minute rocking at RT, water replaced). The gel was then stained (SimplyBlue Safe Stain, LC6060, Thermo Fisher) by microwaving for 45 seconds and

rocking for 5 minutes at RT. Deionized water was used to destain the gel (rocking overnight, RT) before imaging (PhotoDoc-It; Analytik Jena, Jena, Germany).

Western blotting

Gels for western blotting were transferred to a 0.2 mm PVDF membrane (1704156, Bio-Rad Laboratories) using the Trans-Blot Turbo Transfer System (1704150, Bio-Rad Laboratories) and run at 2.5 A for 7 min. Membranes were blocked (5% dry milk in tris-buffered saline with 0.1% Tween buffer) for 1 hour and then incubated overnight in a 1:1000 dilution of a polyclonal anti-der p 2 (AA 18-146) antibody (ABIN7141165, Antibodies-online Inc., Limerick, PA). Following primary antibody incubation, the membranes were washed and incubated in 1:2000 dilution with horseradish peroxidase-conjugated secondary anti-rabbit antibody (#7074, Cell Signaling Technology, Danvers, MA). Enhanced chemiluminescence (ECL) Prime Western Blotting Detection Reagent (Cytiva, Marlborough, MA) was used to for HRP-induced chemiluminescence, and the resulting signals were imaged using an Amersham Imager 680 (GE Life Sciences, Marlborough, MA).

Proteomic analysis

Proteins were removed from the MWCNT surface by incubation with 5% SDS buffer for 5 minutes at 95°C. A 660 nm assay was used to determine protein concentrations prior to submission for proteomic analysis. Individual bands for proteomic analysis were excised from the polyacrylamide gels and submitted without further processing.

The compositions of the protein coronas on MWCNTs were determined using liquid chromatography with tandem mass spectrometry (LC-MS/MS). Proteomic analysis was conducted by the Proteomics and Metabolomics Core Facility, part of the Duke Center for Genomics and Computational Biology. A UPLC column (75 µm x 250 mm, nanoAcquity, Waters Corporation; 400 nL/min) with a 60 minute elution time was used for NanoFlow liquid chromatography with an acetonitrile gradient (5-40%) and 0.1% formic acid. In-line tandem mass spectrometry was used to analyze peptide fragments (Orbitrap Fusion Lumos, Thermo Fisher). We analyzed the LC-MS/MS data using MaxQuant (v2.1.0, Max Planck Institute, Munich, Germany).[54, 55] The raw LC-MS/MS spectra were searched using the integrated Andromeda search engine against the Swiss-Prot *Dermatophagoides pteronyssinus* (European house dust mite; #6956) and *Bos taurus* (bovine; #9913) canonical protein databases from UniProt, accessed on June 5th, 2023. A custom contaminants file was used while searching, which contained a relevant subset of the Common Repository of Adventitious Proteins (cRAP) database.[56] For protein and peptide quantification and identification, default MaxQuant parameters were used including a 0.01 false discovery rate, a minimum peptide length of 7 amino acids, a maximum peptide length of 25 amino acids, oxidation and acetyl groups as variable modifications, and carbamidomethyl as a fixed modification.

Perseus (v2.0.3.1, Max Planck Institute) was used to analyze and filter proteomic data.[57] Proteins were excluded if they were contaminants, quality control standards, or were not observed in at least 2 samples. A quantitative internal standard was not used for these experiments. The intensities of all proteins identified within a sample were summed to

obtain the relative abundance of each protein within each sample triplicate. Averages and standard deviations were calculated from the abundances of the sample triplicates. The mass spectrometry proteomics data have been deposited to the ProteomeXchange Consortium via the Proteomics Identification Database (PRIDE) partner repository with the dataset identifier PXDxxxx and xxxx/PXDxxxx.[58]

Results and Discussion

MWCNT characterization

The diameter of the MWCNTs was measured from TEM images (Fig. 1). Dynamic light scattering is not suitable for these filamentous, non-spherical samples. The MWCNTs have an average diameter of 11.9 ± 0.6 nm (n=6), in good agreement with previous TEM experiments showing a diameter of 12 nm.[14] XPS analysis of MWCNTs revealed a composition of 98.33% carbon, 1.49% oxygen, and 0.18% aluminum (Table 1). A previous analysis of these MWCNTs with XPS found similar levels of carbon (97.8%) and oxygen (1.4%).[14] Trace amounts of aluminum are attributed to the synthesis process, in which metal oxides are present during catalytic chemical vapor deposition.[3, 59-62]

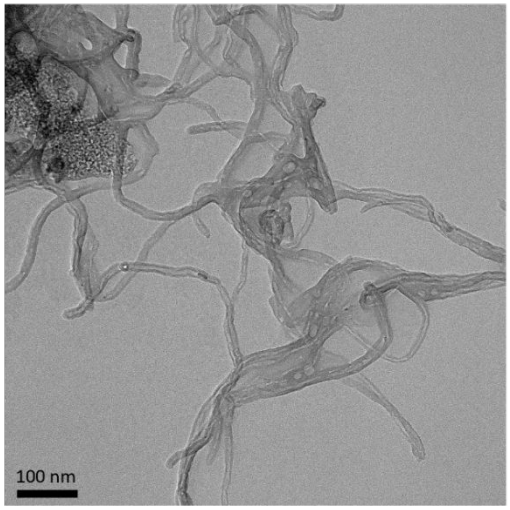

Fig. 1 Representative TEM image of MWCNTs.

Table 1. XPS analysis of MWCNTs with and without a HDM corona present.

Sample	Elemental Analysis (%)				
	C	O	Al	N	Na
MWCNT	98.33	1.49	0.18	-	-
HDM-MWCNT	72.01	22.08	0.20	2.93	2.31

HDM extract forms a corona on MWCNTs

We first characterized the corona that forms on MWCNTs following incubation with HDM extract using gel electrophoresis (Fig. 2). MWCNTs (1 mg/mL) were incubated with HDM (1 mg/mL) in PBS (30 minutes, RT) then washed to remove unbound protein, as described in Materials and Methods (Fig. 2A and Fig. S1). XPS shows that MWCNTs with a HDM corona (HDM-MWCNT) are similar in composition to the pristine MWCNTs, but with an increase in the percentage of oxygen (22.08%) and the addition of nitrogen (2.93%) and sodium (2.31%) (Table 1), likely reflecting the presence of protein and PBS used to form the protein corona. Gel electrophoresis was used to separate and identify the specific proteins that comprise the HDM-MWCNT corona (Fig. 2B). In comparison to HDM alone, the corona formed on MWCNTs (HDM-MWCNT) shows an increase in the band at ~15 kDa the appearance of a ~12 kDa band. These bands were excised and submitted for proteomics. Based on spectral counts, they were identified to be der p 2 (14 kDa) and der p 30 (12 kDa) (Table S1 and S2). In addition, western blotting confirms the ~15 kDa band is der p 2 (Fig. S2).

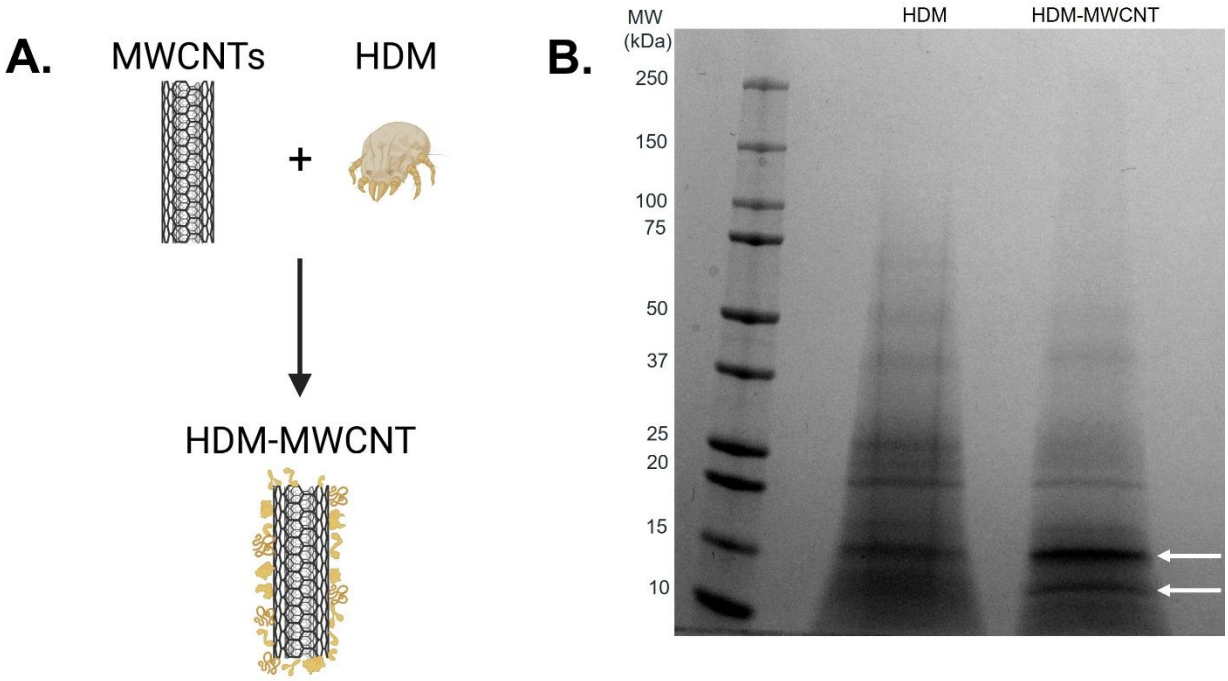

Fig. 2 Formation of a HDM corona on MWCNTs (HDM-MWCNTs). A. Schematic showing the formation of a HDM corona. B. Gel electrophoresis shows the proteins present in HDM compared to the HDM corona formed on MWCNTs. Bands at ~15 kDa and ~12 kDa are highlighted with arrows.

Concentration of the HDM corona

The concentration of HDM proteins that adsorb on the surface of MWCNTs was quantified using a 660 nm protein assay (Fig. 3). MWCNTs (1 mg/mL) were incubated with increasing concentrations of HDM (0.1 mg/mL – 2.0 mg/mL). Samples at lower incubation

concentrations (0.1 mg/mL and 0.25 mg/mL HDM) were pooled (x3) for measurement to provide sufficient protein for the assay. The resulting concentration of protein adsorbed on the MWCNTs increases from 0.1 mg/mL to 0.5 mg/mL and then remains constant with increasing HDM. The maximum concentration of protein in the corona is 7.69 ± 0.80 µg/mg MWCNT, calculated as the average of the samples formed with 0.5-2.0 mg/mL of HDM. This increasing corona concentration as a function of increasing incubation protein concentration is in agreement with other corona studies. Similar assays with polystyrene and silica nanoparticles have shown that increasing the incubation protein concentrations leads to increasing corona concentrations,[63-66] with rare exceptions.[63] However, the maximum corona concentration is low compared to previous studies. For example, titanium nanoparticles incubated with fetal bovine serum form a corona of 50 µg protein/mg of titanium dioxide nanoparticles.[32] It is possible that HDM, which is a mixture of mites, nymphs, fecal matter, and eggs,[37] results in maximum corona formation at relatively low corona concentrations values. In comparison, much of the previous work has focused on human plasma or bovine serum relevant to cell culture and biomedical applications.

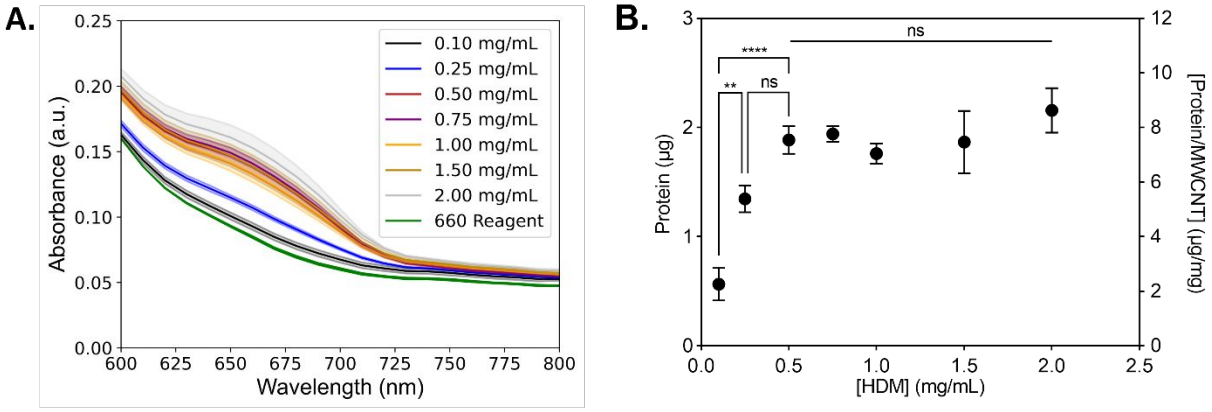

Fig. 3 Protein concentration of the HDM corona formed on MWCNTs. A. MWCNTs were incubated with increasing concentrations of HDM (0.5 mg/mL - 2 mg/mL). The concentration of the resulting corona was measured with a colorimetric protein assay (660 nm assay; n=3 distinct samples). Solid lines show the mean and shading shows the standard deviation. Low concentration samples (0.1 mg/mL and 0.25 mg/mL) were pooled for measurement (x3). B. Protein concentration of the resulting corona. The low concentration samples (0.1 mg/mL and 0.25 mg/mL) are plotted at their n=1 value. Significance was calculated using an ANOVA with a post-hoc Tukey test. ** $p<0.01$, **** $p<0.0001$, ns = not significant.

Composition of the HDM corona

Although gel electrophoresis provides a visualization of the corona proteins (Fig. 2B), proteomics provides a more detailed description of the composition of the protein corona (Table 2). Proteomic analysis is shown as the normalized abundance for HDM alone and the HDM corona (HDM-MWCNT). 79 proteins were identified in HDM and 46 proteins were identified in the HDM-MWCNT coronas. The top-10 of each sample (n=3) are listed.

Previous proteomics studies of HDM alone have identified a complex mixture of proteins.[39, 40] Der p 30, der p 2, der p 36, der p 1, and der p 10 have all previously been identified as highly abundant proteins in mite bodies or extracts.[39, 40] Der f 27, observed in *D. farinae*,[40] was not observed at high abundance in *D. pteronyssinus* previously.

We compare the protein abundance in HDM to the corona formed on MWCNTs. For example, der p 30 is the most highly abundant protein (29.3 ± 13.3%) in the HDM extract, but it was observed at very low levels in the corona (1.00 ± 1.51%). Der p 2 is much less abundant in HDM (12.7 ± 9.01%), but the most abundant allergen in the HDM corona (49.6 ± 15.2%). Der p 36 was the second most highly abundant protein in the corona (14.3 ± 0.98%), although not highly abundant in HDM extract (3.73 ± 3.14%), showing that it is enriched in the corona. Der p 1, which, along with der p 2, is a major human allergen,[38, 42] was observed at low abundance in this lot of HDM (1.79 ± 0.54%) and the corona (0.17 ± 0.17%). The same analysis, using a different lot of HDM, also showed der p 2 was the most abundant protein in the corona (51.6 ± 15.6%), although there were lot-to-lot variations in the HDM and resulting corona (Table S3). This lot-to-lot variation in HDM is expected based on previous work.[67]

A direct comparison of gel electrophoresis and proteomics is complicated by overlapping molecular weights of proteins and different levels of protein staining. For example, based on proteomics data, der p 30 is highly abundant in HDM extract (29.3 ± 13.3%), but difficult to resolve in the gel (Fig. 2B). Gel electrophoresis of the corona results in fewer fragments and a cleaner gel resulting in a visible band at 12 kDa, although the abundance of der p 30 is relatively low (1.00 ± 1.51%) by proteomics. Proteomics of the excised bands at 12 kDa and 15 kDa confirms the presence of der p 30 in the corona and the enrichment of der p 2 (Fig. 2B and Tables S1 and S2).

Overall, the comparison between HDM and HDM-MWCNTs shows that der p 2 is highly concentrated on the surface of MWCNTs, which may be important for allergic airway disease. Der p 1, which is the other major human allergen, was not identified in the protein corona.[38, 41, 42]

Table 2. Normalized abundance (% of total protein) of the top-10 proteins identified in HDM and the HDM corona formed on MWCNTs (HDM-MWCNT). Proteins are ordered by abundance in HDM. Proteins present in a sample, but not in the top-10, are shown in italics. Proteins with normalized abundance < 0.1% are not shown. The most abundant protein in each sample is bolded. Mean and standard deviation are reported (n=3 distinct samples). For allergens, the biochemical name from the WHO/IUIS database is provided in parentheses.

Protein	MW (kDa)	HDM (%)	HDM-MWCNT (%)
Der p 30 (ferritin)	12	**29.3 ± 13.3**	1.00 ± 1.51
Uncharacterized protein LOC113797715	191	18.1 ± 6.71	*0.39 ± 0.29*
Der p 2 (NPC2 family)	14	12.7 ± 9.01	**49.6 ± 15.2**
Fatty acid-binding protein-like	15	5.97 ± 4.61	7.49 ± 9.79
Der p 36 (C2 domain containing protein)	25	3.73 ± 3.14	14.3 ± 0.98

Der f 27 (serpin)	47	2.03 ± 0.85	1.16 ± 1.34
Der p 1 (cysteine protease)	24	1.79 ± 0.54	*0.17 ± 0.17*
Der p 10 (tropomyosin)	33	1.69 ± 1.53	3.90 ± 3.89
Peptidase 1-like	39	1.62 ± 0.31	-
Fructose-bisphosphate aldolase	39	1.44 ± 2.35	-
Nucleoside diphosphate kinase	18	*0.91 ± 0.68*	4.03 ± 0.66
Der p 7 (bactericidal permeability increasing-like)	24	*0.12 ± 0.067*	3.09 ± 1.09
Der f 22 (Group 2-like)	18	-	2.46 ± 3.04
Der p 40 (thioredoxin-like)	12	-	1.10 ± 0.76

Interaction of HDM-MWCNTs with lung fluid proteins

The results above describe the protein corona formed when HDM proteins adsorb on the surface of MWCNTs. The most relevant human exposure to these HDM-MWCNT complexes is through inhalation. To probe this exposure mechanism, we investigated the interaction of BALF with MWCNTs and HDM-MWCNTs. As a first step, we confirmed that a BALF corona formed on pristine MWCNTs. Gel electrophoresis and a protein concentration assay were used to analyze the composition and concentration of the BALF protein corona (Fig. 4). A BALF corona concentration of 35.3 ± 0.85 μg protein/mg MWCNT was measured. Albumin (69 kDa) was the most abundant protein in BALF and in the BALF corona (BALF-MWCNT) in agreement with previous work using proteomics to characterize the protein corona formed on MWCNTs incubated with BALF (24 hrs, 37 °C, 0.1% Pluronic).[68] At high BALF concentrations, two other bands are visible in both BALF and the BALF corona at ~15 kDa and ~8 kDa, along with a low molecular weight smear.

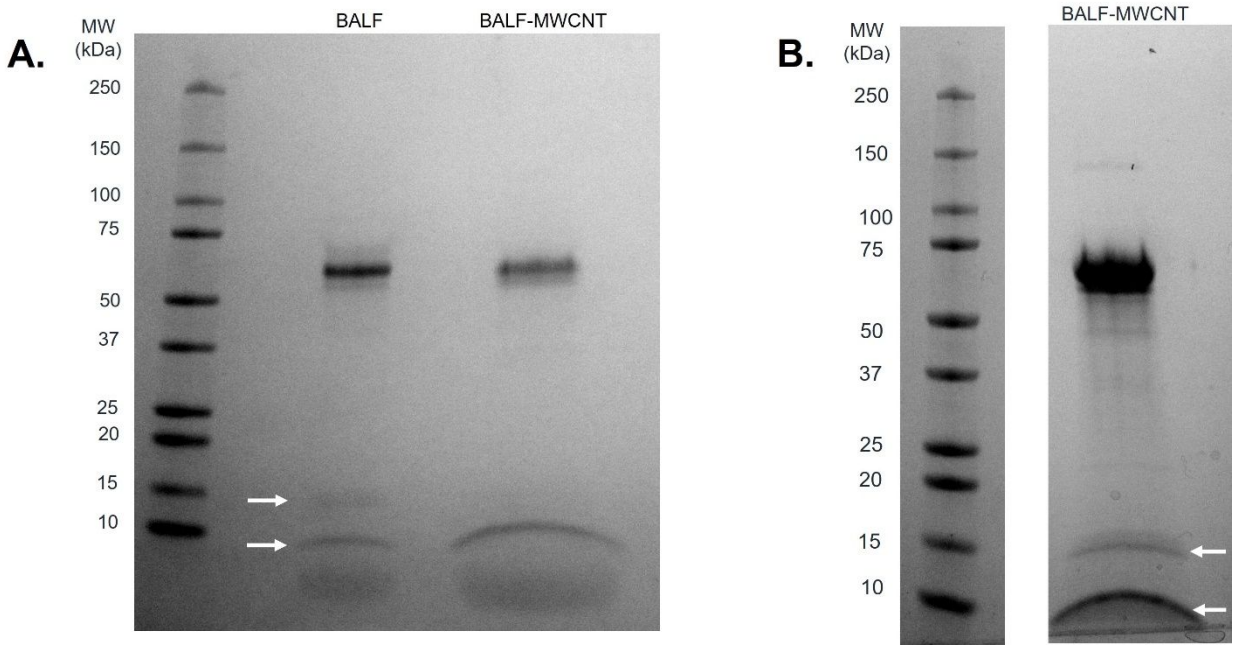

Fig. 4 Gel electrophoresis shows the proteins present in BALF and a corona formed from BALF (BALF-MWCNT). A. Albumin is visible at 69 kDa. Bands at ~15 kDa and ~8 kDa are highlighted with arrows. B. A highly concentrated BALF-MWCNT sample makes the bands at ~15 kDa and ~8 kDa visible (arrows).

We then investigated the interaction of BALF with HDM-MWCNTs. For these experiments, we formed sequential protein coronas by first preparing HDM-MWCNTs and then incubating the HDM-MWCNTs with BALF to form a HDM-BALF-MWCNT corona (Fig. 5). Although the reverse corona (BALF-HDM-MWCNT) is less likely to be formed in a realistic setting, we also generated these coronas for comparison. Gel electrophoresis was used to visualize these sequential coronas (Fig. 6).

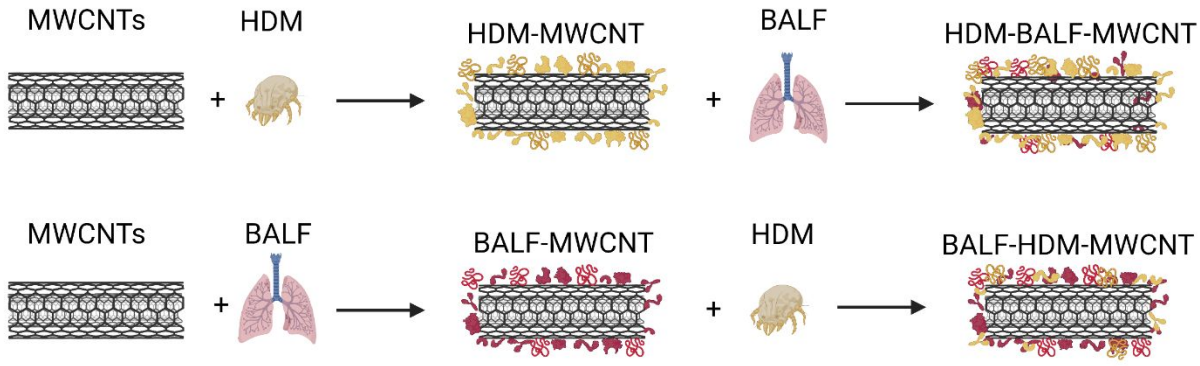

Fig. 5 Schematic showing the formation of sequential coronas formed from HDM and BALF incubated with MWCNTs. The protein listed first is the initial protein used to form the corona.

Gel electrophoresis shows that an initial HDM corona on MWCNTs will result in a HDM-BALF-MWCNT corona with a band at ~70 kDa (likely albumin), as well as ~15 kDa and ~8 kDa (Fig. 6). A 12 kDa, possibly der p 30, is very faint. An initial BALF corona results in a BALF-HDM-MWCNT corona with similar bands to HDM-BALF-MWCNT, but different relative intensities (Fig. 6). The ~15 kDa band dominates HDM-BALF-MWCNT and the ~70 kDa band dominates BALF-HDM-MWCNT.

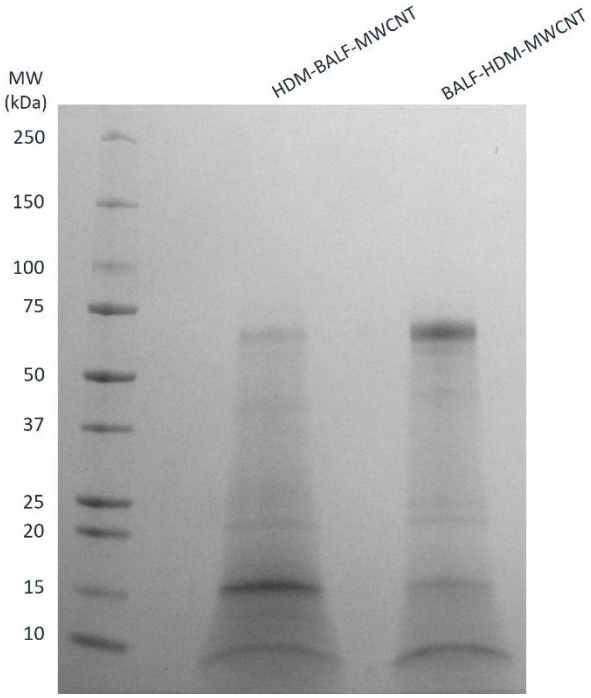

Fig. 6 Gel electrophoresis was used to compare the proteins present in coronas formed sequentially from HDM and BALF (HDM-BALF-MWCNT and BALF-HDM-MWCNT). The protein listed first is the initial protein used to form the corona.

Interaction of HDM-MWCNTs with albumin

Gel electrophoresis following the incubation of HDM-MWCNTs with BALF suggests that der p 2 is present in the HDM-BALF-MWCNT coronas and is not displaced from the surface of MWCNTs by the proteins present in BALF (Fig. 6). To probe this observation, we used albumin, specifically bovine serum albumin (BSA, 66 kDa), as a representative BALF protein. The use of this single representative protein, instead of the BALF mixture, makes proteomics tractable. Repeating the formation of sequential coronas, now using BSA in place of BALF, shows a similar result. An initial HDM corona leads to a HDM-dominated corona (bands at ~15 kDa and ~12 kDa) with a faint ~70 kDa band. An initial BSA corona leads to a complex corona dominated by a ~70 kDa band and previously unobserved proteins (Fig. 7). Der p 2 (14 kDa) is not clearly visible in the BSA-HDM-MWCNT sample.

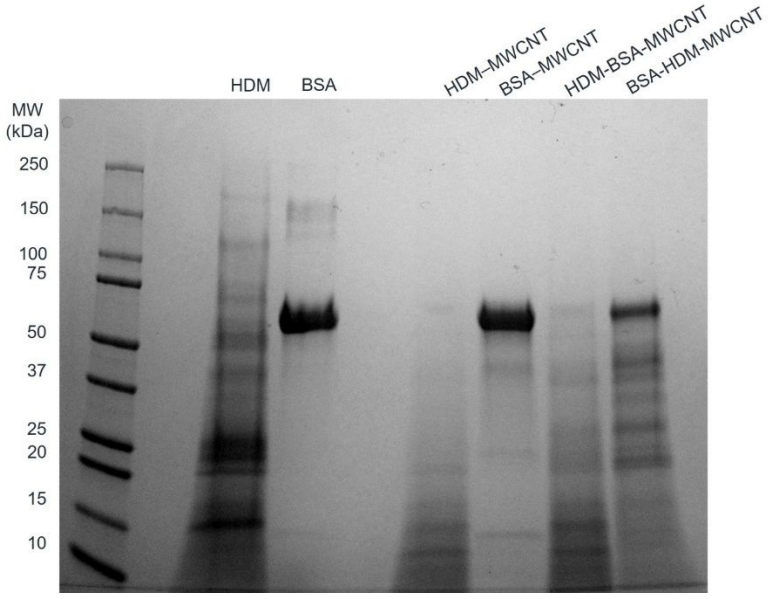

Fig. 7 Gel electrophoresis was used to compare the proteins present in HDM alone, BSA alone, a HDM corona (HDM-MWCNT), a BSA corona (BSA-MWCNT), and sequential coronas (HDM-BSA-MWCNT and BSA-HDM-MWCNT). The protein listed first is the initial protein used to form the corona.

The proteomics data shows that the HDM-BSA-MWCNT corona contains a high concentration of albumin (39.7 ± 4.38%) and der p 2 (36.0 ± 2.91%) (Table 3, Fig. 8). Der p 30 is present at low levels (0.781 ± 0.81%). These results with BSA are in good agreement with the BALF gel electrophoresis experiments (HDM-BALF-MWCNT; Fig. 6), which showed a strong band at ~15 kDa, similar to the molecular weight of der p 2 (14 kDa) and no clear der p 30 band (12 kDa).

The BSA-HDM-MWCNT corona is less physiologically relevant as we expect the MWCNTs to be exposed to HDM and then lung fluid. The initial exposure to BSA leads to an albumin-dominated corona (98.1 ± 0.72%) with a unique collection of HDM corona proteins (Table 3). Der p 2 was not detected in the BSA-HDM-MWCNT coronas, suggesting albumin inhibits the binding of der p 2 binding to the MWCNT surface. This points towards potential surface treatments for MWCNTs that could mitigate any enhanced allergic response. The BALF-HDM-MWCNT gel electrophoresis did show a band at ~15 kDa, but it is likely that this is a BALF protein (Fig. 4).

Table 3. Normalized abundance (% of total protein) of top-5 proteins identified in HDM-BSA-MWCNT and BSA-HDM-MWCNT coronas. Proteins are ordered by abundance in HDM-BSA-MWCNT. Proteins present in a sample, but not in the top-5, are shown in italics. Proteins with normalized abundance < 0.1% are not shown. The most abundant protein is bolded. Mean and standard deviation are reported (n=3 distinct samples). For allergens, the biochemical name from the WHO/IUIS database is provided in parentheses.

Protein	MW (kDa)	HDM-BSA-MWCNT (%)	BSA-HDM-MWCNT (%)
Albumin	**69**	**39.7 ± 4.38**	**98.1 ± 0.72**
Der p 2 (NPC2 family)	14	36.0 ± 2.91	*0.129 ± 0.10*
Der f 22 (Group 2-like)	18	4.37 ± 6.44	-
Fatty acid-binding protein-like	15	3.52 ± 1.75	-
Nucleoside diphosphate kinase	18	2.82 ± 1.76	-
Der p 30 (ferritin)	12	*0.781 ± 0.81*	0.293 ± 0.50
Probable methylmalonate-semialdehyde dehydrogenase	59	-	0.293 ± 0.32
Der p 11 (paramyosin)	102	*1.15 ± 0.61*	0.129 ± 0.02
Probable serine/threonine-protein kinase	191	-	0.130 ± 0.084

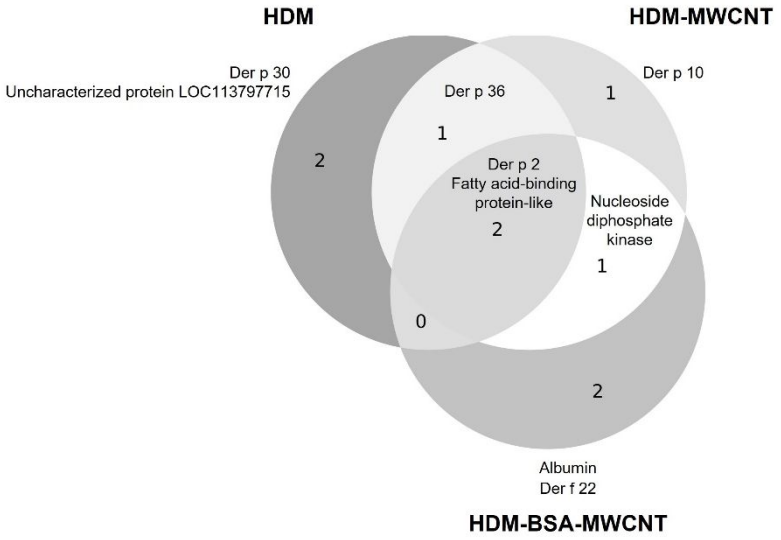

Fig. 8 A Venn diagram shows the overlap of the top-5 proteins present in HDM extract alone, HDM-MWCNTs, HDM-BSA-MWCNTs. The two common proteins in all three samples are der p 2 and fatty acid-binding protein-like.

Conclusions

This work aimed to model real-world exposures to MWCNTs by considering the interaction of HDM proteins with MWCNTs. A combination of XPS (Table 1), gel electrophoresis (Fig. 2), protein concentration assay (Fig. 3), western blotting (Fig. S2), and proteomics (Table 2 and Table S1 and S2) shows that HDM proteins adsorb on the surface of MWCNTs forming a protein corona, similar to the coronas observed for nanomaterials used in biomedical applications.[29, 69-71] Much previous work has focused on serum proteins. The protein corona dictates the subsequent biological response to these nanomaterials. It is likely that the HDM corona will similarly determine the cellular and *in vivo* response to HDM-MWCNTs. We find that der p 2, a major HDM allergen,[42] becomes highly concentrated on the surface of MWCNTs, which may be important for allergic airway disease. When the HDM-MWCNTs are then exposed to BALF or BSA (Fig.

5), which serves as a representative lung fluid protein, we find that der p 2 remains highly abundant (36.0 ± 2.91% with BSA) (Fig. 6, Fig. 7, Table 3). This shows that der p 2 is not displaced from the surface of MWCNTs by lung fluid proteins and suggests that any physiological response due to the highly concentrated der p 2 will not be mitigated by lung fluid, although future functional assays will be necessary to probe the allergic potential of der p 2 adsorbed on the surface of MWCNTs. Previous *in vivo* experiments showed that mice co-exposed to MWCNTs and HDM extract displayed increased eosinophilic lung inflammation that was not observed with MWCNTs or HDM alone,[72] suggesting der p 2 is functional. The results described in this manuscript suggest that the high local concentration of der p 2 on the MWCNTs may deliver the allergen to immune cells exacerbating allergic lung inflammation. Future work will extend these studies to MWCNTs following common purification methods and chemical functionalizations to determine if these results are general. In addition, a variety of carbon-based nanomaterials present in the environment (ultrafine particulate matter, wildfire smoke) exacerbate asthma.[73, 74] Our findings may have broad implications for understanding the underlying mechanism.

Ethics Declarations

Conflicts of interest

The authors declare that they have no conflicts of interest.

Funding

This study received funding from the NIH-NIEHS (5R01ES032443). This material is based upon work supported by the National Science Foundation Graduate Research Fellowship under DGE 2139754.

Acknowledgments

We thank the Duke University School of Medicine for the use of the Proteomics and Metabolomics Shared Resource, which provided proteomics service, with special thanks to Erik Soderblom and Greg Waitt for technical advice. TEM was performed at the Chapel Hill Analytical and Nanofabrication Laboratory, CHANL, a member of the North Carolina Research Triangle Nanotechnology Network (RTNN), which is supported by the National Science Foundation, Grant ECCS-1542015, as part of the National Nanotechnology Coordinated Infrastructure (NNCI).

References

1. V. T. Rathod, J. S. Kumar and A. Jain, Polymer and ceramic nanocomposites for aerospace applications, *Appl. Nanosci.*, 2017, **7**, 519-548.
2. *Carbon nanotubes: market size, share & trends analysis report by product (SWNT, MWNT), by application (polymers, energy, electrical & electronics), and segment forecasts, 2015 - 2022*, San Francisco, CA, 2022.
3. K. Donaldson, R. Aitken, L. Tran, V. Stone, R. Duffin, G. Forrest and A. Alexander, Carbon nanotubes: a review of their properties in relation to pulmonary toxicology and workplace safety, *Toxicol. Sci.*, 2006, **92**, 5-22.
4. J. P. Ryman-Rasmussen, M. F. Cesta, A. R. Brody, J. K. Shipley-Phillips, J. I. Everitt, E. W. Tewksbury, O. R. Moss, B. A. Wong, D. E. Dodd and M. E. Andersen, Inhaled carbon nanotubes reach the subpleural tissue in mice, *Nat. Nanotechnol.*, 2009, **4**, 747-751.
5. I. G. Canu, K. Batsungnoen, A. Maynard and N. Hopf, State of knowledge on the occupational exposure to carbon nanotubes, *Int. J. Hyg. Environ. Health*, 2020, **225**, 113472.
6. M. D. Wright, A. J. Buckley and R. Smith, Estimates of carbon nanotube deposition in the lung: improving quality and robustness, *Inhal. Toxicol.*, 2020, **32**, 282-298.
7. J. Muller, F. Huaux, N. Moreau, P. Misson, J.-F. Heilier, M. Delos, M. Arras, A. Fonseca, J. B. Nagy and D. Lison, Respiratory toxicity of multi-wall carbon nanotubes, *Toxicol. Appl. Pharmacol.*, 2005, **207**, 221-231.
8. D. W. Porter, A. F. Hubbs, R. R. Mercer, N. Wu, M. G. Wolfarth, K. Sriram, S. Leonard, L. Battelli, D. Schwegler-Berry and S. Friend, Mouse pulmonary dose- and time course-responses induced by exposure to multi-walled carbon nanotubes, *Toxicology*, 2010, **269**, 136-147.
9. M. F. Cesta, J. P. Ryman-Rasmussen, D. G. Wallace, T. Masinde, G. Hurlburt, A. J. Taylor and J. C. Bonner, Bacterial lipopolysaccharide enhances PDGF signaling and pulmonary fibrosis in rats exposed to carbon nanotubes, *Am. J. Respir. Cell Mol. Biol.*, 2010, **43**, 142-151.
10. J. P. Ryman-Rasmussen, E. W. Tewksbury, O. R. Moss, M. F. Cesta, B. A. Wong and J. C. Bonner, Inhaled multiwalled carbon nanotubes potentiate airway fibrosis in murine allergic asthma, *Am. J. Respir. Cell Mol. Biol.*, 2009, **40**, 349-358.
11. K.-i. Inoue, E. Koike, R. Yanagisawa, S. Hirano, M. Nishikawa and H. Takano, Effects of multi-walled carbon nanotubes on a murine allergic airway inflammation model, *Toxicol. Appl. Pharmacol.*, 2009, **237**, 306-316.
12. E. M. Rydman, M. Ilves, A. J. Koivisto, P. A. Kinaret, V. Fortino, T. S. Savinko, M. T. Lehto, V. Pulkkinen, M. Vippola and K. J. Hämeri, Inhalation of rod-like carbon nanotubes causes unconventional allergic airway inflammation, *Part. Fibre Toxicol.*, 2014, **11**, 1-17.
13. S. G. Han, R. Andrews and C. G. Gairola, Acute pulmonary response of mice to multi-wall carbon nanotubes, *Inhal. Toxicol.*, 2010, **22**, 340-347.
14. A. J. Taylor-Just, M. D. Ihrie, K. S. Duke, H. Y. Lee, D. J. You, S. Hussain, V. K. Kodali, C. Ziemann, O. Creutzenberg and A. Vulpoi, The pulmonary toxicity of carboxylated or aminated multi-walled carbon nanotubes in mice is determined by the prior purification method, *Part. Fibre Toxicol.*, 2020, **17**, 1-18.

15. K. S. Duke, A. J. Taylor-Just, M. D. Ihrie, K. A. Shipkowski, E. A. Thompson, E. C. Dandley, G. N. Parsons and J. C. Bonner, STAT1-dependent and-independent pulmonary allergic and fibrogenic responses in mice after exposure to tangled versus rod-like multi-walled carbon nanotubes, *Part. Fibre Toxicol.*, 2017, **14**, 1-15.
16. *OSHA Fact Sheet: Working safely with nanomaterials*, U.S. Department of Labor, Washington D.C.
17. H. Y. Lee, D. J. You, A. J. Taylor-Just, L. Tisch, R. D. Bartone, H. M. Atkins, L. M. Ralph, S. Antoniak and J. C. Bonner, Role of the protease-activated receptor-2 (PAR2) in the exacerbation of house dust mite-induced murine allergic lung disease by multi-walled carbon nanotubes, *Particle Fibre Toxicol.*, 2023, **20**, 32.
18. E. D. Kuempel, M.-C. Jaurand, P. Møller, Y. Morimoto, N. Kobayashi, K. E. Pinkerton, L. M. Sargent, R. C. Vermeulen, B. Fubini and A. B. Kane, Evaluating the mechanistic evidence and key data gaps in assessing the potential carcinogenicity of carbon nanotubes and nanofibers in humans, *Crit. Rev. Toxicol.*, 2017, **47**, 1-58.
19. A. V. Singh, P. Laux, A. Luch, C. Sudrik, S. Wiehr, A.-M. Wild, G. Santomauro, J. Bill and M. Sitti, Review of emerging concepts in nanotoxicology: Opportunities and challenges for safer nanomaterial design, *Toxicol. Mech. Methods*, 2019, **29**, 378-387.
20. M. Nicoletti, C. Capodanno, C. Gambarotti and E. Fasoli, Proteomic investigation on bio-corona of functionalized multiwalled carbon nanotubes, *Biochim. Biophys. Acta Gen. Subj.*, 2018, **1862**, 2293-2303.
21. L. García-Hevia, M. Saramiforoshani, J. Monge, N. Iturrioz-Rodríguez, E. Padín-González, F. González, L. González-Legarreta, J. González and M. L. Fanarraga, The unpredictable carbon nanotube biocorona and a functionalization method to prevent protein biofouling, *J. Nanobiotech.*, 2021, **19**, 1-13.
22. X. Cai, R. Ramalingam, H. San Wong, J. Cheng, P. Ajuh, S. H. Cheng and Y. W. Lam, Characterization of carbon nanotube protein corona by using quantitative proteomics, *Nanomed. Nanotech. Biol. Med.*, 2013, **9**, 583-593.
23. K. Bhattacharya, S. P. Mukherjee, A. Gallud, S. C. Burkert, S. Bistarelli, S. Bellucci, M. Bottini, A. Star and B. Fadeel, Biological interactions of carbon-based nanomaterials: From coronation to degradation, *Nanomed. Nanotech. Biol. Med.*, 2016, **12**, 333-351.
24. C. C. Fleischer and C. K. Payne, Nanoparticle-cell interactions: Molecular structure of the protein corona and cellular outcomes, *Acc. Chem. Res.*, 2014, **47**, 2651-2659.
25. C. D. Walkey and W. C. W. Chan, Understanding and controlling the interaction of nanomaterials with proteins in a physiological environment, *Chem. Soc. Rev.*, 2012, **41**, 2780-2799.
26. M. P. Monopoli, C. Åberg, A. Salvati and K. A. Dawson, Biomolecular coronas provide the biological identity of nanosized materials, *Nat. Nanotechnol.*, 2012, **7**, 779-786.
27. K. Nienhaus and G. U. Nienhaus, Towards a molecular-level understanding of the protein corona around nanoparticles–recent advances and persisting challenges, *Curr. Opin. Biomed. Eng.*, 2019, **10**, 11-22.

28. L. Kobos and J. Shannahan, Biocorona-induced modifications in engineered nanomaterial–cellular interactions impacting biomedical applications, *WIRES Nanomed. Nanobio.*, 2020, **12**, e1608.
29. C. K. Payne, A protein corona primer for physical chemists, *J. Chem. Phys.*, 2019, **151**, 130901.
30. P. C. Ke, S. Lin, W. J. Parak, T. P. Davis and F. Caruso, A decade of the protein corona, *ACS Nano*, 2017, **11**, 11773-11776.
31. H. Whitwell, R.-M. Mackay, C. Elgy, C. Morgan, M. Griffiths, H. Clark, P. Skipp and J. Madsen, Nanoparticles in the lung and their protein corona: the few proteins that count, *Nanotox.*, 2016, **10**, 1385-1394.
32. K. M. Poulsen, M. C. Albright, N. J. Niemuth, R. M. Tighe and C. K. Payne, Interaction of TiO2 nanoparticles with lung fluid proteins and the resulting macrophage inflammatory response, *Environ. Sci. Nano*, 2023.
33. W. R. Thomas, B. J. Hales and W.-A. Smith, House dust mite allergens in asthma and allergy, *Trends Mol. Med.*, 2010, **16**, 321-328.
34. A. Jacquet, The role of innate immunity activation in house dust mite allergy, *Trends Mol. Med.*, 2011, **17**, 604-611.
35. M. A. Calderón, A. Linneberg, J. Kleine-Tebbe, F. De Blay, D. H. F. de Rojas, J. C. Virchow and P. Demoly, Respiratory allergy caused by house dust mites: what do we really know?, *J. Allergy Clin. Immunol.*, 2015, **136**, 38-48.
36. T. A. Platts-Mills, A. L. de Weck, R. Aalberse, J. Bessot, B. Bjorksten, E. Bischoff, J. Bousquet, J. Van Bronswijk, G. ChannaBasavanna and M. Chapman, Dust mite allergens and asthma—a worldwide problem, *J. Allergy Clin. Immunol.*, 1989, **83**, 416-427.
37. W. R. Thomas, W.-A. Smith, B. J. Hales, K. L. Mills and R. M. O'Brien, Characterization and immunobiology of house dust mite allergens, *Int. Arch. Allergy Immunol.*, 2002, **129**, 1-18.
38. M. D. Chapman and T. Platts-Mills, Purification and characterization of the major allergen from Dermatophagoides pteronyssinus-antigen P1, *J. Immun.*, 1980, **125**, 587-592.
39. R. Waldron, J. McGowan, N. Gordon, C. McCarthy, E. B. Mitchell and D. A. Fitzpatrick, Proteome and allergenome of the European house dust mite Dermatophagoides pteronyssinus, *PLoS One*, 2019, **14**, e0216171.
40. V. Bordas-Le Floch, M. Le Mignon, L. Bussières, K. Jain, A. Martelet, V. Baron-Bodo, E. Nony, L. Mascarell and P. Moingeon, A combined transcriptome and proteome analysis extends the allergome of house dust mite Dermatophagoides species, *PLoS One*, 2017, **12**, e0185830.
41. M. Reithofer and B. Jahn-Schmid, Allergens with protease activity from house dust mites, *Int. J. Mol. Sci.*, 2017, **18**, 1368.
42. M. Weghofer, W. Thomas, G. Pittner, F. Horak, R. Valenta and S. Vrtala, Comparison of purified Dermatophagoides pteronyssinus allergens and extract by two-dimensional immunoblotting and quantitative immunoglobulin E inhibitions, *Clin. Exp. Allergy*, 2005, **35**, 1384-1391.
43. W. R. Thomas, T. K. Heinrich, W.-A. Smith and B. J. Hales, Pyroglyphid house dust mite allergens, *Protein Pept. Lett.*, 2007, **14**, 943-953.

44. K. Meno, P. B. Thorsted, H. Ipsen, O. Kristensen, J. N. Larsen, M. D. Spangfort, M. Gajhede and K. Lund, The crystal structure of recombinant proDer p 1, a major house dust mite proteolytic allergen, *J. Immunol.*, 2005, **175**, 3835-3845.
45. S. De Halleux, E. Stura, L. VanderElst, V. Carlier, M. Jacquemin and J.-M. Saint-Remy, Three-dimensional structure and IgE-binding properties of mature fully active Der p 1, a clinically relevant major allergen, *J. Allergy Clin. Immunol.*, 2006, **117**, 571-576.
46. M. Chruszcz, M. D. Chapman, L. D. Vailes, E. A. Stura, J.-M. Saint-Remy, W. Minor and A. Pomés, Crystal structures of mite allergens Der f 1 and Der p 1 reveal differences in surface-exposed residues that may influence antibody binding, *J. Mol. Biol.*, 2009, **386**, 520-530.
47. U. Derewenda, J. Li, Z. Derewenda, Z. Dauter, G. Mueller, G. Rule and D. Benjamin, The crystal structure of a major dust mite allergen Der p 2, and its biological implications, *J. Mol. Biol.*, 2002, **318**, 189-197.
48. Park, Lee, Lee, Ree, Hong and Yong, Localization of a major allergen, Der p 2, in the gut and faecal pellets of Dermatophagoides pteronyssinus, *Clin. Exp. Allergy*, 2000, **30**, 1293-1297.
49. M. D. Ihrie, K. S. Duke, K. A. Shipkowski, D. J. You, H. Y. Lee, A. J. Taylor-Just and J. C. Bonner, STAT6-dependent exacerbation of house dust mite-induced allergic airway disease in mice by multi-walled carbon nanotubes, *NanoImpact*, 2021, **22**, 100309.
50. I. Radauer-Preiml, A. Andosch, T. Hawranek, U. Luetz-Meindl, M. Wiederstein, J. Horejs-Hoeck, M. Himly, M. Boyles and A. Duschl, Nanoparticle-allergen interactions mediate human allergic responses: protein corona characterization and cellular responses, *Part. Fibre Toxicol.*, 2015, **13**, 1-15.
51. E. Kuijpers, C. Bekker, W. Fransman, D. Brouwer, P. Tromp, J. Vlaanderen, L. Godderis, P. Hoet, Q. Lan and D. Silverman, Occupational exposure to multi-walled carbon nanotubes during commercial production synthesis and handling, *Ann. Occ. Hyg.*, 2016, **60**, 305-317.
52. B. Nowack, R. M. David, H. Fissan, H. Morris, J. A. Shatkin, M. Stintz, R. Zepp and D. Brouwer, Potential release scenarios for carbon nanotubes used in composites, *Environ. Int.*, 2013, **59**, 1-11.
53. C. A. Schneider, W. S. Rasband and K. W. Eliceiri, NIH Image to ImageJ: 25 years of image analysis, *Nat. Methods*, 2012, **9**, 671-675.
54. J. Cox and M. Mann, MaxQuant enables high peptide identification rates, individualized ppb-range mass accuracies and proteome-wide protein quantification, *Nat. Biotechnol.*, 2008, **26**, 1367-1372.
55. S. Tyanova, T. Temu and J. Cox, The MaxQuant computational platform for mass spectrometry-based shotgun proteomics, *Nat. Protoc.*, 2016, **11**, 2301-2319.
56. cRAP protein sequences: The Global Proteome Machine; 2012).
57. S. Tyanova, T. Temu, P. Sinitcyn, A. Carlson, M. Y. Hein, T. Geiger, M. Mann and J. Cox, The Perseus computational platform for comprehensive analysis of (prote) omics data, *Nat. Methods*, 2016, **13**, 731-740.
58. Y. Perez-Riverol, A. Csordas, J. Bai, M. Bernal-Llinares, S. Hewapathirana, D. J. Kundu, A. Inuganti, J. Griss, G. Mayer and M. Eisenacher, The PRIDE database

and related tools and resources in 2019: improving support for quantification data, *Nucl. Acids Res.*, 2019, **47**, D442-D450.

59. *R. P. Silvy, C. Pirlot and B. Culot, Catalyst system for a multi-walled carbon nanotube production process,* 2011, U.S. Patent No. 7,923,615.
60. *R. P. Silvy, F. Liegeois, B. Culot and S. Lambert, Method of synthesising a support catalyst for the production of carbon nanotubes,* 2010, U.S. Patent No. 7,754,181.
61. A.-C. Dupuis, The catalyst in the CCVD of carbon nanotubes—a review, *Prog. Mater. Sci.*, 2005, **50**, 929-961.
62. C. M. White, R. Banks, I. Hamerton and J. F. Watts, Characterisation of commercially CVD grown multi-walled carbon nanotubes for paint applications, *Prog. Org. Coat.*, 2016, **90**, 44-53.
63. M. P. Monopoli, D. Walczyk, A. Campbell, G. Elia, I. Lynch, F. B. Bombelli and K. A. Dawson, Physical-chemical aspects of protein corona: relevance to in vitro and in vivo biological impacts of nanoparticles, *J. Am. Chem. Soc.*, 2011, **133**, 2525-2534.
64. K. Partikel, R. Korte, N. C. Stein, D. Mulac, F. C. Herrmann, H.-U. Humpf and K. Langer, Effect of nanoparticle size and PEGylation on the protein corona of PLGA nanoparticles, *Eur. J. Pharm. Biopharm.*, 2019, **141**, 70-80.
65. C. Gräfe, A. Weidner, M. vd Lühe, C. Bergemann, F. H. Schacher, J. H. Clement and S. Dutz, Intentional formation of a protein corona on nanoparticles: Serum concentration affects protein corona mass, surface charge, and nanoparticle–cell interaction, *Int. J. Biochem. Cell Biol.*, 2016, **75**, 196-202.
66. K. M. Poulsen and C. K. Payne, Concentration and composition of the protein corona as a function of incubation time and serum concentration: an automated approach to the protein corona, *Anal. Bioanal. Chem.*, 2022, **414**, 7265-7275.
67. J. M. Cyphert-Daly, Z. Yang, J. L. Ingram, R. M. Tighe and L. G. Que, Physiologic response to chronic house dust mite exposure in mice is dependent on lot characteristics, *J. Allergy Clin. Immunol.*, 2019, **144**, 1428-1432. e1428.
68. G. M. Hilton, PhD, North Carolina State University, 2017.
69. S. Runa, M. Hussey and C. K. Payne, Nanoparticle–cell interactions: Relevance for public health, *J. Phys. Chem. B*, 2018, **122**, 1009-1016.
70. J. Shannahan, The biocorona: a challenge for the biomedical application of nanoparticles, *Nanotechnol. Rev.*, 2017, **6**, 345-353.
71. D. Docter, S. Strieth, D. Westmeier, O. Hayden, M. Gao, S. K. Knauer and R. H. Stauber, No king without a crown–impact of the nanomaterial-protein corona on nanobiomedicine, *Nanomedicine*, 2015, **10**, 503-519.
72. M. D. Ihrie, A. J. Taylor-Just, N. J. Walker, M. D. Stout, A. Gupta, J. S. Richey, B. K. Hayden, G. L. Baker, B. R. Sparrow and K. S. Duke, Inhalation exposure to multi-walled carbon nanotubes alters the pulmonary allergic response of mice to house dust mite allergen, *Inhal. Toxicol.*, 2019, **31**, 192-202.
73. O. K. Kurt, J. Zhang and K. E. Pinkerton, Pulmonary health effects of air pollution, *Curr. Opin. Pulm. Med.*, 2016, **22**, 138.
74. C. E. Reid, M. Brauer, F. H. Johnston, M. Jerrett, J. R. Balmes and C. T. Elliott, Critical review of health impacts of wildfire smoke exposure, *Environ. Health Perspect.*, 2016, **124**, 1334-1343.